

## X-RAY DECLINE AND REJUVENATION OF A RECURRENT NOVA

HIROSHI ITOH

Department of Astronomy, Kyoto University

AND

IZUMI HACHISU

Department of Aeronautical Engineering, Kyoto University

Received 1989 August 11; accepted 1990 February 2

### ABSTRACT

The dynamical evolution and nonequilibrium X-ray emission of recurrent-nova remnants have been investigated by using a spherically symmetric hydrodynamic code. We assume that the nova ejecta expand into a wind from a red-giant companion. The wind material is blast shocked, and emits copious X-rays. The blast shock soon breaks out of the wind region which has formed since the previous outburst, and the remnant undergoes nearly unimpeded expansion. The rarefaction and adiabatic cooling of the remnant result in a drastic decline in the X-ray emission. At this stage the recombination exceeds the ionization, and the X-ray spectrum is characterized by strong recombination lines and continua. The blast shock eventually catches up with the relatively slow ejecta of the previous outbursts. The X-ray emission may then be rejuvenated in both luminosity and spectral shape. Observations of such an X-ray decline and rejuvenation may provide a clue to the outburst mechanism of recurrent novae.

*Subject headings:* shock waves — stars: novae — stars: X-rays — X-rays: binaries

### I. INTRODUCTION

Two mechanisms have been proposed for recurrent-nova outbursts: a thermonuclear runaway (TNR) model and a main-sequence accretor model (e.g., Webbink *et al.* 1987). The TNR model resembles the widely accepted TNR model of classical novae, except that the companion of the white dwarf is a red giant instead of a low-mass, main-sequence star (see Starrfield 1988 and Shara 1989 for reviews). In order for the outburst to recur every 10 years or so, however, the mass accretion rate has to be high and the white dwarf has to be both massive and luminous in comparison with those in classical-nova systems. The accreted material then cannot cool enough to become strongly degenerated before ignition, and the resulting outbursts are expected to be much weaker than the outbursts of classical novae. This prediction may be in conflict with strong outbursts observed in some recurrent novae. The strong outbursts may be due to a drastic enhancement of mass transfer from a red giant to a main-sequence star (Webbink *et al.* 1987).

X-ray observations play an important role in the study of recurrent-nova outbursts. It has long been known from optical observations that some recurrent-nova systems are associated with a dense circumbinary medium (CBM), which is most likely formed by the wind from the red giant between outbursts (see Rosino 1987 for a review). By interacting with nova ejecta having expansion velocities of several hundred or several thousand  $\text{km s}^{-1}$ , the CBM will be shock-heated to X-ray-emitting temperatures (Brecher, Ingham, and Morrison 1977). The X-ray emission from RS Ophiuchi during the latest outburst in 1985 (Mason *et al.* 1987), the detection of which was the first in recurrent novae during the outburst, has been interpreted in terms of the shocked-CBM scenario (Bode and Kahn 1985; Mason *et al.* 1987; O'Brien, Kahn, and Bode 1987).

The blast shock eventually breaks out of the CBM into a rarefied ambient medium. The shocked CBM then undergoes an almost free expansion and, as a result of rarefaction and

adiabatic cooling, the X-ray emission will fall sharply (Brecher, Ingham, and Morrison 1977). A steep decline of X-ray emission has been observed in RS Ophiuchi during the 1985 outburst (Mason *et al.* 1987). Observations of the X-ray luminosity and spectrum and of their time developments will give us important information about the outburst energy, the mass-loss rate of the red giant, the wind velocity, and so on.

After the CBM's steep decline in X-ray emission, the blackbody radiation from the hot surface of the erupted white dwarf may show up in the X-ray spectrum. The detection of this blackbody spectrum will constitute compelling evidence for the TNR model. It will also provide constraints on the model of the delayed mass ejection from the white dwarf. In classical novae, the explosive mass ejection is known to be followed by a quasi-steady, optically thick wind from the white dwarf with the luminosity being close to the Eddington limit (e.g., Sparks, Starrfield, and Truran 1978; Kato and Hachisu 1988). Soft X-ray emission intensifies as the photosphere contracts (Ögelman, Krautter, and Beuermann 1987).

The delayed and relatively slow mass ejection from a previous eruption of the star may have formed a slowly expanding gaseous shell around the stellar system; such a shell has actually been found around T Pyxidis (see Shara *et al.* 1989 and references therein). The shell will be hit by the blast shock which has broken out of the CBM, and will be heated to emit X-rays. A reverse shock will be reflected from the shell and reheat the CBM.

In the present paper, we investigate the time development of the X-ray emission from a recurrent-nova remnant sketched above. The evolutionary stage in which the blast shock propagates through the CBM has been investigated by Brecher, Ingham, and Morrison (1977), Bode and Kahn (1985), O'Brien, Kahn, and Bode (1987), and O'Brien and Kahn (1987). These authors derived analytical expressions for the dynamical evolution, and considered the X-ray emission under the assumption of coronal ionization equilibrium. We use a numerical code in the investigation of the dynamical evolution, and take

account of the electron-ion temperature nonequilibrium and the ionization nonequilibrium in the calculation of the X-ray spectrum. Further, we extend the investigation to the evolutionary stages in which the blast shock breaks out of the CBM and hits the gaseous shell. It should be noted here that supernovae may undergo a similar breakout from a dense circumstellar medium (Itoh and Fabian 1984; Band and Liang 1988; Itoh and Masai 1989). Also, the collision of the blast shock with a high-density region some distance away from the explosion site has been investigated for several remnants including SN 1572 and SN 1987A (Dickel and Jones 1985; Itoh *et al.* 1987; Masai *et al.* 1987, 1988; Itoh 1988; Chevalier and Liang 1989). Because of the relatively short time scales involved in the evolution of recurrent novae, the study of recurrent novae will also help us understand the evolution of young supernova remnants.

In the next section, we describe the physical assumptions used in the model calculations. Numerical results are presented in § III. Their implications for the observations and proposed outburst mechanisms of recurrent novae are discussed in § IV. A summary is given in the final section.

## II. THE MODELS

### a) Initial Conditions

The incipient expansion of recurrent-nova ejecta should depend on the outburst mechanism. This mechanism is presently controversial. Here we assume that the ejecta have a total mass  $M_0$ , and spherically expand with a total kinetic energy  $E_0$ . The expansion velocity,  $v$ , is taken to be proportional to the distance,  $r$ , from the center of the expansion. Although negative velocity gradients have been observed in classical novae, they are not prominent in the initial ejecta of recurrent novae (Friedjung 1987). The density profile,  $\rho(r)$ , of the initial ejecta is taken to be uniform from the center out to a radius  $r_c$ . For the outer regions, we assume a power law,  $\rho(r_c)(r/r_c)^{-n}$ , with a constant index  $n$  out to a surface at a radius  $r_0$ . Such a ramp in density may be formed when the shock propagates down the density gradients in the envelope and immediate surroundings of the erupting star. The delayed mass ejection mentioned in the previous section is not considered for the initial ejecta, since it does not affect the early interaction of the ejecta with the CBM.

The red-giant companion is assumed to generate a spherically symmetric, steady wind between the outbursts. The density profile of the resulting CBM may be written as

$$\rho(r) = \dot{M}/4\pi r^2 W, \quad (1)$$

where  $\dot{M}$  is the mass-loss rate of the red giant, and  $W$  is the wind velocity. Although the orbital motion of the red giant may result in the CBM being more extensive in the orbital plane than in the perpendicular direction, we ignore this effect for simplicity. The total mass and outer radius of the CBM are written as

$$M_{\text{cbm}} = \dot{M} T, \quad (2)$$

and

$$r_{\text{cbm}} = W T, \quad (3)$$

respectively, where  $T$  is the time elapsed since the previous outburst.

The density in the immediate vicinity of the CBM is likely to be much lower than that in the CBM. We assume that a rela-

tively small mass,  $M_s$ , is uniformly distributed from the radius  $r_{\text{cbm}}$  out to a radius  $r_{\text{shell}}$ . At  $r = r_{\text{shell}}$ , a shell of a mass  $M_{\text{shell}}$  and of a uniform density  $\rho_{\text{shell}}$  is assumed to have been formed by the delayed and relatively slow mass ejection from the previous outburst(s). The density outside the shell is taken to be uniform at  $\rho_0$ . A temperature of  $10^4$  K is assumed everywhere. The initial expansion velocities of the CBM and the ambient media are much lower than those of the ejecta, and are ignored in the numerical calculations.

### b) Hydrodynamics and X-Ray Emission

The dynamical evolution of the recurrent-nova remnant is calculated from the equations of mass, momentum, and energy conservation for a spherically symmetric flow. The Lagrangian equations are written in explicit finite-difference form with an artificial viscosity as prescribed by Richtmyer and Morton (1967). Test calculations have shown that 40, 50, 20, 20, and 50 zones suffice for the ejecta, the CBM, the adjacent low-density region, the shell, and the surrounding medium, respectively. In the course of the numerical calculation, the zone width becomes very small in the outer region of the cool ejecta, and we merge such zones to relax the Courant condition. The electron and ion temperatures are treated separately. On the basis of the plasma measurements at the Earth's bow shock (Bame *et al.* 1979), we assume that only ions are heated at the shock front through collisionless processes. Electrons are assumed to be heated through Coulomb collisions (Spitzer 1962) with ions in the postshock region. The possibility of substantial electron heating at the fast collisionless shock front (McKee 1974) is ignored in the present calculations (see also Itoh, Masai, and Nomoto 1988).

We assume that hydrogen and helium are completely ionized everywhere, and calculate the time-dependent ionization of carbon, nitrogen, oxygen, neon, sodium, magnesium, aluminum, silicon, sulfur, argon, calcium, iron, and nickel. Since we are interested in highly charged ions which can emit X-rays efficiently, only the ionization stages  $\text{C}^{2+}$ ,  $\text{N}^{2+}$ ,  $\text{O}^{2+}$ ,  $\text{Ne}^{2+}$ ,  $\text{Na}^{5+}$ ,  $\text{Mg}^{3+}$ ,  $\text{Al}^{6+}$ ,  $\text{Si}^{3+}$ ,  $\text{S}^{3+}$ ,  $\text{Ar}^{3+}$ ,  $\text{Ca}^{5+}$ ,  $\text{Fe}^{5+}$ , and  $\text{Ni}^{5+}$ , and higher ionization stages of the same atoms are considered. The ionization and recombination coefficients are taken from Arnaud and Rothenflug (1985) and references therein.

The nonequilibrium state of ionization is used in the calculation of the X-ray spectrum. The radiation code (provided by K. Masai) uses spectral line data which are taken from Mewe, Gronenschild, and van den Oord (1985) and are modified by Masai; this version includes collisional excitation, innershell ionization, dielectronic recombination, and radiative recombination. For the continuum emission, thermal bremsstrahlung, radiative recombination into  $n \leq 3$  levels of hydrogenic, He-like, and Li-like ions, and two-photon decay from  $2s(2S)$  levels of hydrogenic ions and  $1s2s(1S)$  levels of He-like ions are taken into account. We adopt the cosmic abundances of elements (Allen 1973) for the CBM. For the other regions, we set the mass fractions of hydrogen and helium equal to 0.58 and 0.40, respectively, and those of the heavier elements to the cosmic values.

The nonequilibrium X-ray emission is also calculated for the evaluation of the radiative cooling. Since this is very time consuming, the radiative cooling is considered only for the nova ejecta having electron temperatures higher than  $10^5$  K in most of the models presented in the next section. The radiative cooling is relatively unimportant outside the ejecta. We ignore

TABLE 1  
MODEL PARAMETERS<sup>a</sup>

Model	$M_0$ ( $10^{-6} M_\odot$ )	$E_0$ ( $10^{44}$ ergs)	$M_{\text{cbm}}$ ( $10^{-6} M_\odot$ )
A.....	1	1	1
B.....	1	1	3
C.....	0.1	0.1	1

<sup>a</sup> For the parameters that are common among the models, see the text.

the cooling by gas-grain collisions, although the nova ejecta and the CBM may be dusty. The ultraviolet radiation and X-rays from the erupted star are also ignored; although these emissions will significantly affect the ionization state and thermal balance of the relatively cool gas, they will have little effect on the X-ray emitting gas. Thermal conduction is also ignored.

### c) Calculated Models

We have calculated three models (A, B, and C) by varying the value(s) of  $M_0$ ,  $E_0$ , or  $M_{\text{cbm}}$  as summarized in Table 1. The adopted values of  $M_0$  sandwich an estimate of  $5 \times 10^{-7} M_\odot$  for the 1958 outburst of RS Ophiuchi (Pottasch 1967; Snijders 1987). The value of  $E_0$  is chosen so that the resulting maximum expansion velocity of the initial ejecta,  $4.2 \times 10^3 \text{ km s}^{-1}$ , is consistent with the measurements for RS Ophiuchi at optical, ultraviolet, and radio wavelengths (see, e.g., Bode 1987; Porcas, Davis, and Graham 1987; Taylor *et al.* 1989). The mass of the CBM is taken to be equal to or greater than that of the ejecta.

The remaining parameters are common among the three models. In each case, we assume that the ejecta expand freely until their outer boundary meets the CBM, and start the numerical calculation by setting  $r_0 = 10^{13} \text{ cm}$ . This value for  $r_0$  is of the same order as the separation between the binary components of RS Ophiuchi (Livio, Truran, and Webbink 1986). The values of  $r_c$  and  $n$  are arbitrarily set equal to  $9.1 \times 10^{12} \text{ cm}$  and 12, respectively. Since the mass contained between radii  $r_c$  and  $r_0$  is taken to be much smaller than  $M_{\text{cbm}}$ , the numerical results are insensitive to the value of  $n$ . For the CBM, we assume  $r_{\text{cbm}} = 10^{15} \text{ cm}$ . For the latest outburst of RS Ophiuchi, relations (2) and (3) with  $T = 17 \text{ yr}$  yield plausible values for  $\dot{M}$  ( $= 5.9 \times 10^{-8} M_\odot \text{ yr}^{-1}$  in models A and C and  $1.8 \times 10^{-7} M_\odot \text{ yr}^{-1}$  in model B) and  $W$  ( $= 19 \text{ km s}^{-1}$ ). The parameters for the matter outside the CBM are taken to be  $M_a = 10^{-7} M_\odot$ ,  $r_{\text{shell}} = 7 \times 10^{15} \text{ cm}$ ,  $M_{\text{shell}} = 10^{-6} M_\odot$ ,  $\rho_{\text{shell}} = 5 \times 10^3 \text{ amu cm}^{-3}$ , and  $\rho_0 = 10^{-1} \text{ amu cm}^{-3}$ .

Figure 1 shows the radial distributions of the density and velocity at time  $t = 0.31$  days after the outburst in model A. In model B the density of the CBM is higher than that shown in Figure 1 by a factor of 3, while in model C the density of the ejecta is lower by a factor of 10.

## III. NUMERICAL RESULTS

We first describe the numerical results for model A in some detail. Subsequently we present the results for models B and C to examine the effects of increasing the density of the CBM and lowering both the ejected mass and the outburst energy.

### a) Model A

#### i) Expansion in the CBM

The collision of the ejecta with the CBM gives rise to two shock waves: a blast shock into the CBM and a reverse shock

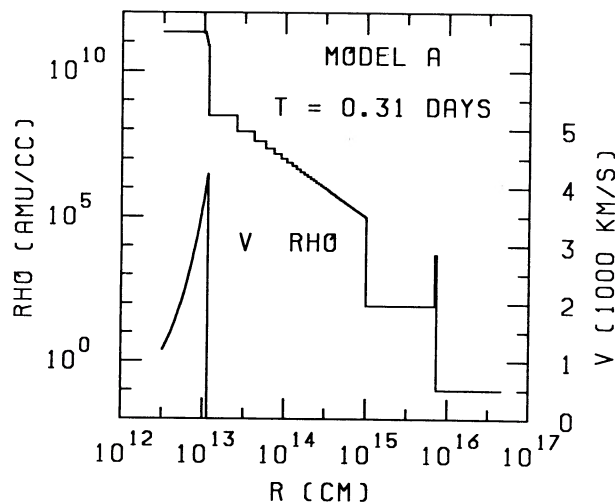


FIG. 1.—The radial profiles of the density (labeled RHO) and velocity (V) at  $t = 0.31$  days in model A. The surface of the ejecta is at a radius of  $1.13 \times 10^{13} \text{ cm}$ , the outer boundary of the CBM at  $10^{15} \text{ cm}$ , and the shell at  $7 \times 10^{15} \text{ cm}$ .

into the ejecta. To exemplify the dynamical structure of the nova remnant in this evolutionary stage, Figure 2a shows the radial profiles of the density, velocity, mean temperature ( $T_m$ ) of electrons and ions, and electron temperature ( $T_e$ ) at  $t = 28$  days in model A. A sharp density peak at a radius of  $6.32 \times 10^{14} \text{ cm}$  marks the outermost region of the reverse-shocked ejecta. Since the deceleration of the sharp density peak by the less dense CBM is subject to a Rayleigh-Taylor instability, the shocked ejecta will in reality fragment into many pieces.

The density, velocity, and temperature profiles are qualitatively the same as those in models of young supernova remnants (e.g., Itoh and Masai 1989). The blast-shocked CBM is hotter than the reverse-shocked ejecta. As shown in Figure 1, the density of the initial ejecta is higher than that of the CBM by three orders of magnitude or more. This density contrast, in conjunction with an approximate pressure equilibrium within the remnant, implies a temperature contrast of a similar magnitude across the contact discontinuity between the ejecta and the CBM. The mean temperature rises toward the shock front in both the ejecta and the CBM, since the immediate preshock density decreases with time. The shocked ejecta may cool by radiation, because of the relatively high density and low-postshock temperature. The sharp density peak is due in part to the compression that accompanies the radiative cooling. Thermal instabilities may set in during the radiative cooling to facilitate the fragmentation of the shocked ejecta. The cooling of the shocked ejecta will eventually be balanced with the heating by the ultraviolet radiation and X-rays from the erupted star. Detailed treatment of the thermal evolution of the shocked ejecta would be necessary in studying their optical and ultraviolet emission, but is beyond the scope of the present paper. A separate calculation has been made for the early stages of the evolution by including the radiative cooling of the CBM. The results show that the radiative cooling is insignificant in the blast-shocked CBM in model A.

The X-ray spectrum at  $t = 28$  days in model A is shown in Figure 2b. It has been convolved with a Gaussian to a resolution of  $0.1E^{0.5} \text{ keV}$  (FWHM), where  $E$  is the photon energy in units of keV. The distance and interstellar column density to the remnant are set equal to 1.6 kpc and  $2.4 \times 10^{21}$

H atoms  $\text{cm}^{-2}$ , respectively, which are estimates for RS Ophiuchi (Hjellming *et al.* 1986). The ejecta could absorb some of the X-ray photons produced in the CBM. However, this effect will be significantly reduced by the fragmentation of the shocked ejecta, and therefore it is ignored in the spectral calculations. The absorption by the CBM is also ignored; this is acceptable since the column density of the unshocked CBM is smaller than the interstellar value adopted here when  $t > 1$  day in model A. The most conspicuous feature in the spectrum is an iron  $K\alpha$  emission line blend centered at a photon energy of 6.69 keV, with an equivalent width of 1.45 keV. As indicated by the mean photon energy of the emission feature, iron is mostly ionized to a helium-like stage in the shocked CBM. Lighter elements also emit appreciably in K lines, though they are more fully stripped of their bound electrons than iron. If the CBM were enriched with metal elements, the X-ray lines would be enhanced accordingly.

The averaged electron temperature within the remnant and the 0.1–30 keV luminosity are plotted against time in Figures 3a and 3b, respectively. In order to focus on those regions that contribute to the X-ray emission, we average the electron temperature over the remnant using the bremsstrahlung emissivity as a weighting factor. While the blast shock expands in the CBM, the luminosity of the CBM,  $L_{\text{cbm}}$ , may in principle be estimated by approximating the blast wave by a uniform shell in which the density is higher than the immediate preshock value by a factor of 4. We thus obtain

$$L_{\text{cbm}} = 3 \times 10^{33} (\epsilon/10^{-23} \text{ cm}^3 \text{ ergs s}^{-1}) (M_{\text{cbm}}/10^{-6} M_{\odot})^2 \times (r_{\text{cbm}}/10^{15} \text{ cm})^{-2} (r_{\text{blast}}/10^{15} \text{ cm})^{-1} \text{ ergs s}^{-1}, \quad (4)$$

where  $\epsilon$  is the X-ray emissivity and  $r_{\text{blast}}$  is the blast-shock radius. Unfortunately, however, the evaluation of the emissivity is not straightforward in general, since the emissivity may

be affected appreciably by the departure of the ionization state from equilibrium.

#### ii) Breakout from the CBM

The blast shock breaks out of the CBM at  $t \approx 36$  days in model A. The time of the breakout may be written as

$$t_{\text{break}} = r_{\text{cbm}} / \langle V_{\text{blast}} \rangle, \quad (5)$$

where  $\langle V_{\text{blast}} \rangle$  is the average expansion velocity of the blast shock in the CBM, and may be approximated as

$$\langle V_{\text{blast}} \rangle = \left(\frac{2}{3}\right) [1 + (1 + M_{\text{cbm}}/M_0)^{-1}] (2E_0/M_0)^{1/2}. \quad (6)$$

In equation (6) the shock velocity is assumed to be larger than the velocity of the shocked gas by a factor of four-thirds, the momentum is assumed to be conserved in a given solid angle, and an arithmetic mean of the initial and final velocities is taken. Equations (5) and (6) yield  $t_{\text{break}} = 36$  days for the parameters of model A, in agreement with the numerical result.

After the breakout into the surrounding rarefied medium, the blast shock is accelerated for a while by the pressure gradient in the CBM (Itoh and Fabian 1984; Band and Liang 1988; Itoh and Masai 1989). Thereafter the CBM undergoes nearly unimpeded expansion, and is subject to significant adiabatic cooling as seen in Figure 3a. Consequently, the X-ray emission declines steeply as shown in Figure 3b. The adiabatic cooling of the CBM is so rapid that the recombination lags behind the decline of the electron temperature. The CBM thus becomes over ionized, and the recombination lines and continua, especially those of iron at  $E > 6$  keV, become very conspicuous in the X-ray spectrum, as exemplified in Figure 4

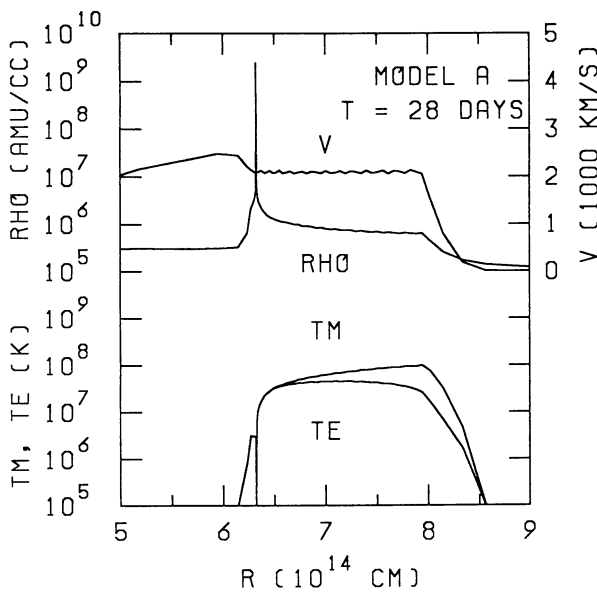


FIG. 2a

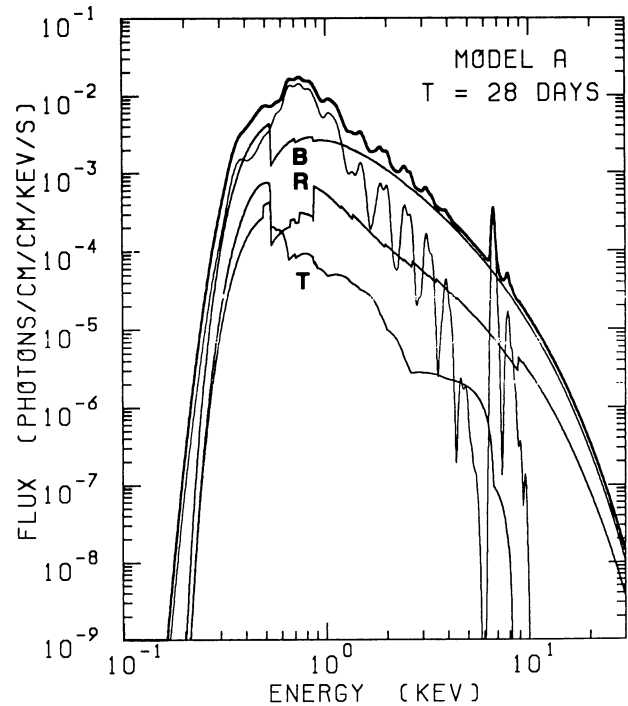


FIG. 2b

FIG. 2.—(a) The radial profiles of the density (labeled RHO), velocity (V), mean temperature (TM), and electron temperature (TE), and (b) the X-ray spectrum, at  $t = 28$  days in model A. The spectrum is shown for the total emission (thick solid line), line emission (thin solid line), bremsstrahlung (B), recombination radiation (R), and two-photon emission (T). The total and line spectra are convolved with a Gaussian to a resolution of  $0.1E^{0.5}$  keV (FWHM). The distance and interstellar column density to the remnant are set equal to 1.6 kpc and  $2.4 \times 10^{21}$  H atoms  $\text{cm}^{-2}$ , respectively, which are estimates obtained for RS Ophiuchi (Hjellming *et al.* 1986). The emission from the central star is not included.

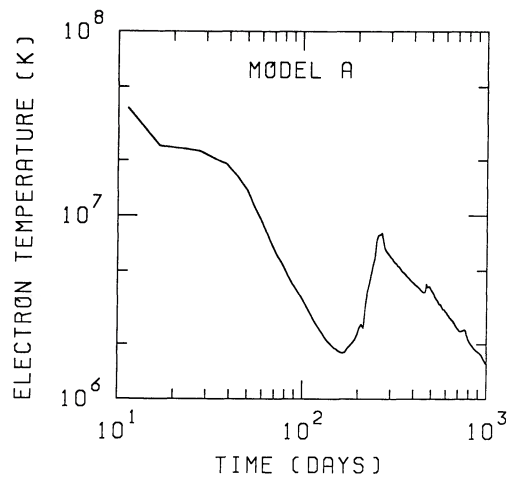


FIG. 3a

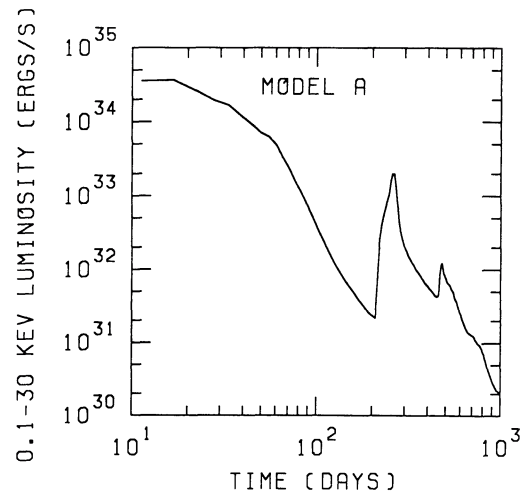


FIG. 3b

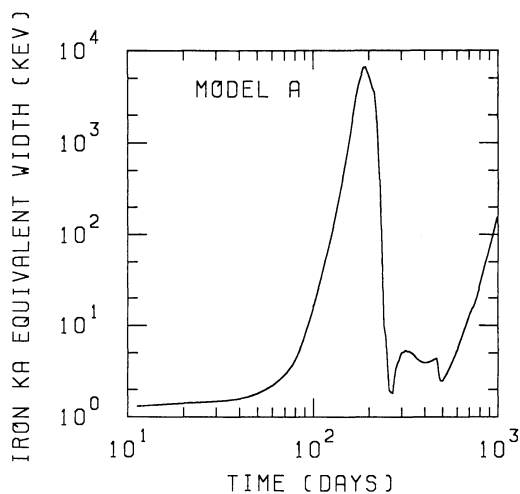


FIG. 3c

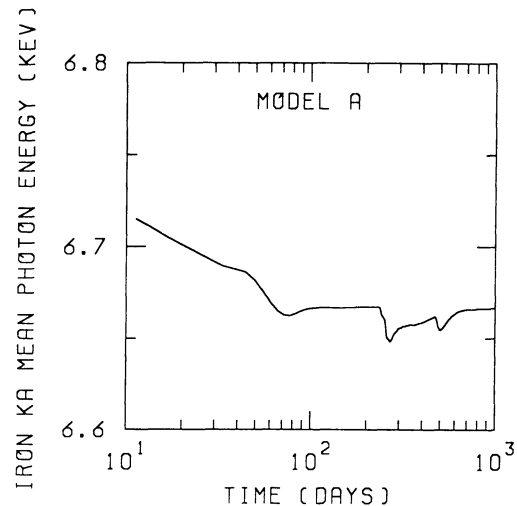


FIG. 3d

FIG. 3.—Time evolution of (a) the averaged electron temperature within the remnant, (b) the 0.1–30 keV luminosity, and (c) the equivalent width and (d) mean photon energy of an iron  $K\alpha$  emission feature, in model A. For the definition of the averaged electron temperature, see the text. The secondary X-ray flare around  $t = 480$  days might be an artifact of the numerical scheme, as discussed in the text.

( $t = 159$  days). The time evolution of the equivalent width and mean photon energy of the iron  $K\alpha$  emission feature is shown in Figures 3c and 3d, respectively. The drastic increase of the equivalent width after the breakout displays the growing departure from ionization equilibrium. For 100 days  $< t < 200$  days, the mean photon energy corresponds approximately to the  $1s2p(^3P) - 1s^2(^1S)$  transition in  $\text{Fe}^{24+}$ , indicating the dominance of the recombination process in the iron  $K\alpha$  emission.

The expansion of the CBM is eventually decelerated by the ambient medium. This is accomplished through propagation of a reverse shock from the contact surface between the two media into the CBM. The second reverse shock reheats the CBM, and leads to an upturn of the averaged electron temperature within the remnant as seen in Figure 3a.

### iii) Collision with the Shell

The blast shock reaches the shell at  $t \approx 210$  days in model A. If the shock expanded at a constant velocity, the time of the collision would be  $(r_{\text{shell}}/r_{\text{cbm}})t_{\text{break}}$ , which is about 250 days in

model A. In reality, the acceleration of the shock immediately after the breakout hastens the collision. As the blast shock moves into the dense shell, the X-ray luminosity increases steeply and the X-ray spectrum changes its shape. The recombination lines and continua emitted from the over-ionized CBM become overwhelmed by the collisionally excited lines and bremsstrahlung continuum from the shocked, under-ionized shell material. The spectrum thus recovers its more conventional shape, as exemplified in Figure 5 ( $t = 258$  days). The line emission is significantly enhanced by the nonequilibrium ionization (e.g., Itoh 1979). The X-ray luminosity attains a local maximum when the transmitted shock reaches the outer boundary of the shell. This maximum may be estimated as

$$L_{\text{shell, max}} = 4 \times 10^{32} (\epsilon/10^{-23} \text{ cm}^3 \text{ ergs s}^{-1}) \\ \times (\rho_{\text{shell}}/10^4 \text{ amu cm}^{-3}) \\ \times (M_{\text{shell}}/10^{-6} M_{\odot}) \text{ ergs s}^{-1}, \quad (7)$$

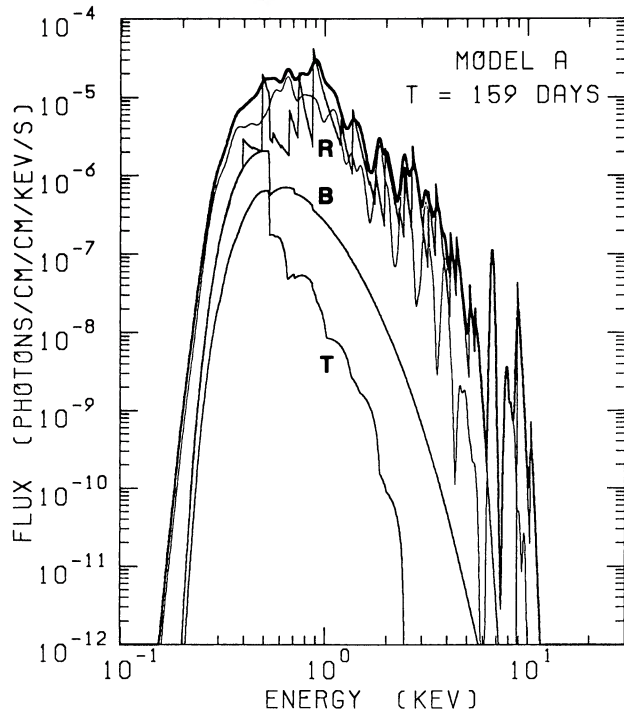


FIG. 4.—Same as Fig. 2b, but at  $t = 159$  days

by assuming that the shell is compressed by a factor of 4. The X-ray luminosity begins to decline at  $t \approx 260$  days, when the blast shock breaks out of the shell.

In addition to the transmitted shock, a reflected (reverse) shock is excited upon collision of the blast shock with the shell. In model A, this third reverse shock overtakes the second one,

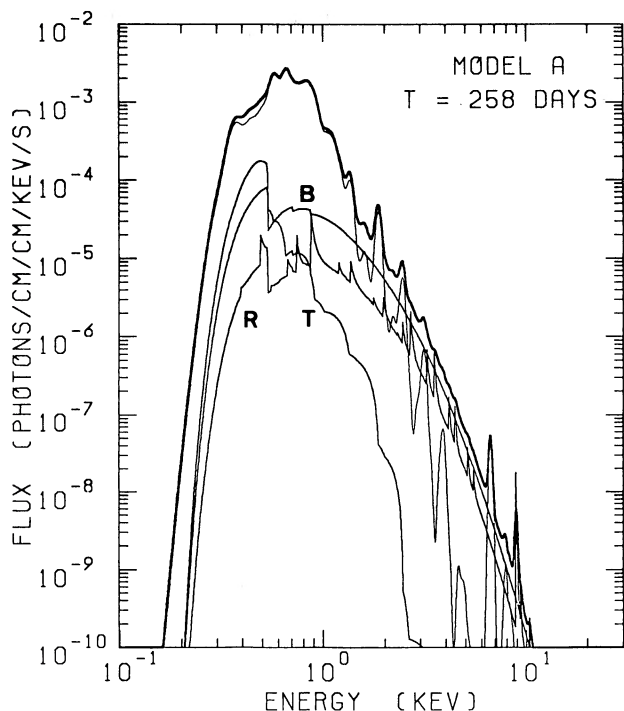


FIG. 5.—Same as Fig. 2b, but at  $t = 258$  days

and reaches the ejecta at  $t \approx 460$  days. As shown in Figure 3b, this collision gives rise to a secondary X-ray flare. We note, however, that the luminosity and spectrum of the rejuvenated ejecta should be sensitive to the density, which is not calculated in detail in our models as mentioned in § IIIa(i). The fragmentation of the shocked ejecta will also affect the luminosity profile of the secondary flare significantly.

#### b) Model B

The CBM of model B is denser and more massive than that of model A by a factor of 3. The averaged electron temperature and 0.1–30 keV luminosity of the remnant, and the equivalent width and mean photon energy of the iron  $K\alpha$  emission feature in model B are plotted against time in Figures 6a, 6b, 6c, and 6d, respectively. Evidently the relatively dense and massive CBM hastens the deceleration of the remnant expansion, and delays the collision with the shell, as seen by comparing Figure 6 and Figure 3. The higher density and mass also lead to enhancement of the X-ray emission before the breakout, as suggested by equation (4). On the other hand, the maximum X-ray luminosity during the primary flare is scarcely affected, because it is determined mainly by the shocked shell. The problematic secondary flare is not seen in Figure 6b, since the reverse shock from the shell has not reached the ejecta as of  $t = 1000$  days in model B.

In model B, the innermost regions of the shocked CBM are dense enough to cool appreciably by radiation. We have made a separate model calculation (model Bm) for  $t \lesssim 31$  days, including the radiative cooling of the CBM. The global properties of the remnant are not much different between models B and Bm. For instance, the averaged electron temperature and 0.1–30 keV luminosity at  $t > 15$  days in model Bm agree with those in model B to within 10%. The X-ray spectra at  $t = 26$  days in models B and Bm are shown in Figures 7a and 7b, respectively; they differ only slightly from each other at  $E < 1$  keV. The equivalent width and mean photon energy of the iron  $K\alpha$  emission feature do not differ appreciably between the two models.

If the density of the CBM is high or the outburst energy low compared with that in model B, the correspondingly high-postshock density or low-postshock temperature may make the bulk of the blast-shocked CBM cool appreciably by radiation. Since the departure from ionization equilibrium may be insignificant in the radiatively cooling gas, the dynamical evolution and X-ray emission of the radiative CBM before the breakout may be calculated semianalytically by assuming the equilibrium emission coefficients (Bode and Kahn 1985; O'Brien, Kahn, and Bode 1987; O'Brien and Kahn 1987).

Since the CBM is formed by a wind from a red giant, it is likely to be dusty. Thus the shocked CBM may also cool significantly through gas-grain collisions. The evaluation of this effect and the calculation of the infrared and X-ray spectra would require taking into account dust destruction through sputtering (e.g., Callus, Evans, and Albinson 1986; Evans 1987; Itoh 1989). These considerations are beyond the scope of the present paper.

#### c) Model C

The ejecta mass and outburst energy of model C are both lower than those of model A by a factor of 10. The averaged electron temperature and 0.1–30 keV luminosity of the remnant, and the equivalent width and mean photon energy of the iron  $K\alpha$  emission feature in model C are plotted against

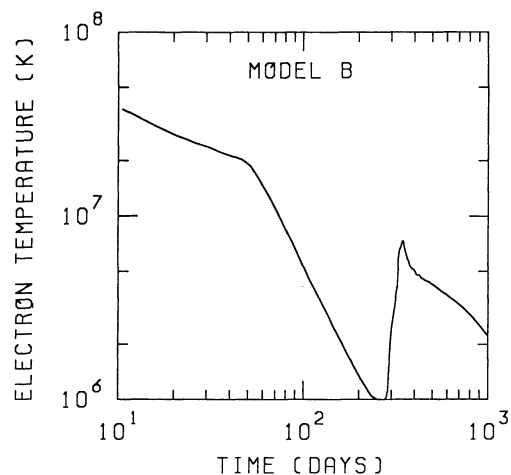


FIG. 6a

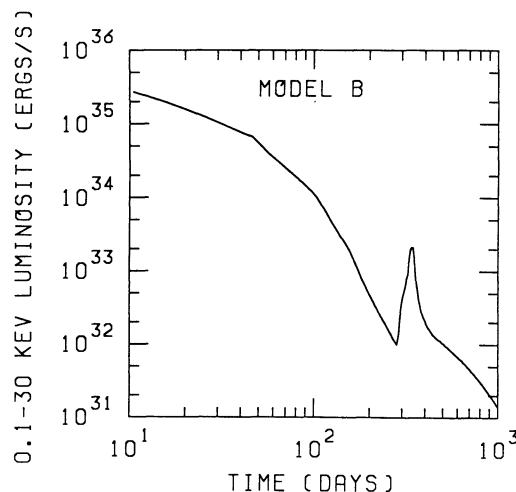


FIG. 6b

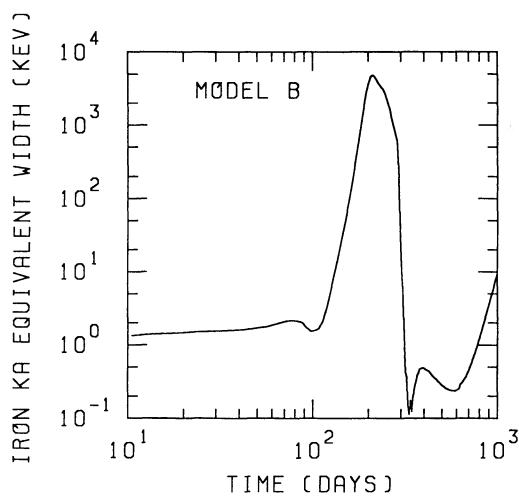


FIG. 6c

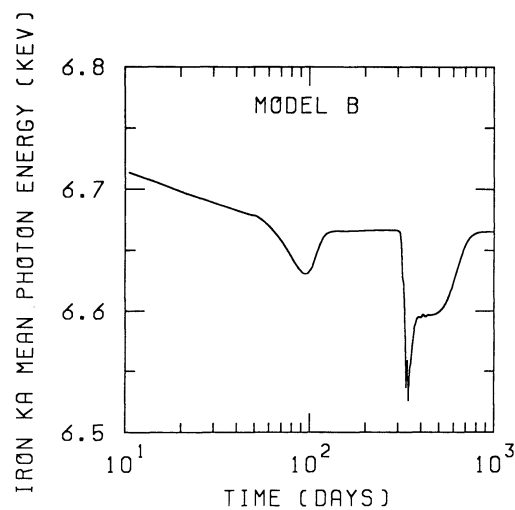


FIG. 6d

FIG. 6.—Same as Figs 3a, 3b, 3c, and 3d, but in model B

time in Figures 8a, 8b, 8c, and 8d, respectively. Because of the low outburst energy, the breakout of the blast shock from the CBM and its collision with the shell occur much later than in model A. The shock heating of the shell is relatively weak in model C, as inferred from a comparison of Figures 8a and 3a. Thus the nonequilibrium X-ray emissivity of the shocked shell material is relatively low, and the maximum X-ray luminosity during the flare is correspondingly low, in model C.

#### IV. DISCUSSION

The breakout of the blast shock from the CBM has distinctive observational consequences, as described above. It is predicted that the breakout is followed by a steep decline in the X-ray emission (Fig. 3b), softening of the spectral shape (Figs. 2b and 4), and prominence of recombination lines and continua in the spectrum (Fig. 4). A rapid decline of the X-ray flux was actually observed between 2 and 3 months after the 1985 outburst of the recurrent nova RS Ophiuchi (Mason *et al.* 1987). Mason *et al.* (1987) interpreted this as being due to the shock breakout. Unfortunately, however, no conclusive evi-

dence was found for (or against) the predicted softening of the X-ray spectrum during the decline (see Fig. 3 of Mason *et al.* 1987). Thus the above interpretation should be tested by spectral observations of the next outburst. It should be noted that the nonthermal radio emission also declined rapidly  $\sim 40$  days after the 1985 outburst (Hjellming *et al.* 1986); the rate of the decline can be shown to be consistent with free expansion of an optically thin synchrotron source.

The rejuvenation of the recurrent-nova remnant via shock collision with a dense shell is also yet to be confirmed by observations. In the recorded outbursts in 1866 and 1946, T Coronae Borealis exhibited secondary brightening  $\sim 106$  days after the primary light maximum (see Kenyon 1986 and Webbink *et al.* 1987 for reviews). The secondary brightening may have been due to the collision of the nova ejecta, expanding at a velocity of  $4500 \text{ km s}^{-1}$ , with the material at a distance of 250 AU away from the stellar system (Gratton 1952). Alternatively, it may also be explained within the context of an accretion-powered outburst model for recurrent novae (Webbink 1976; Webbink *et al.* 1987). The former model pre-

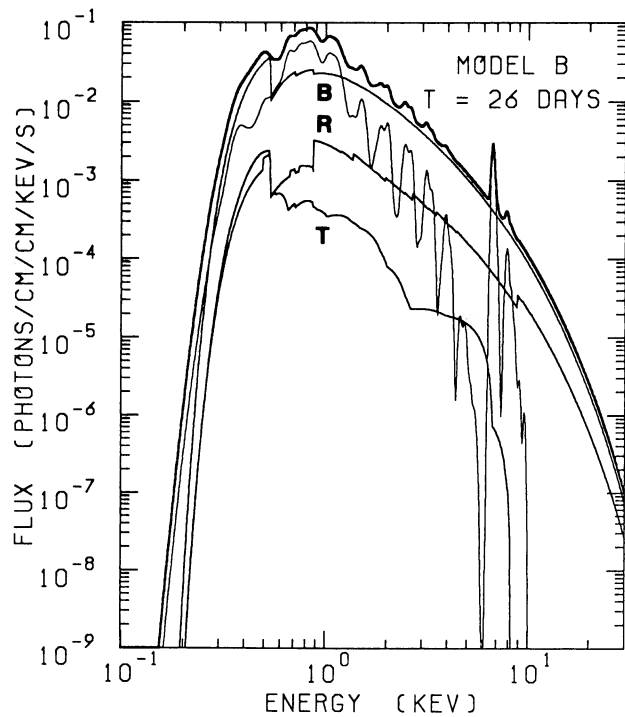


FIG. 7a

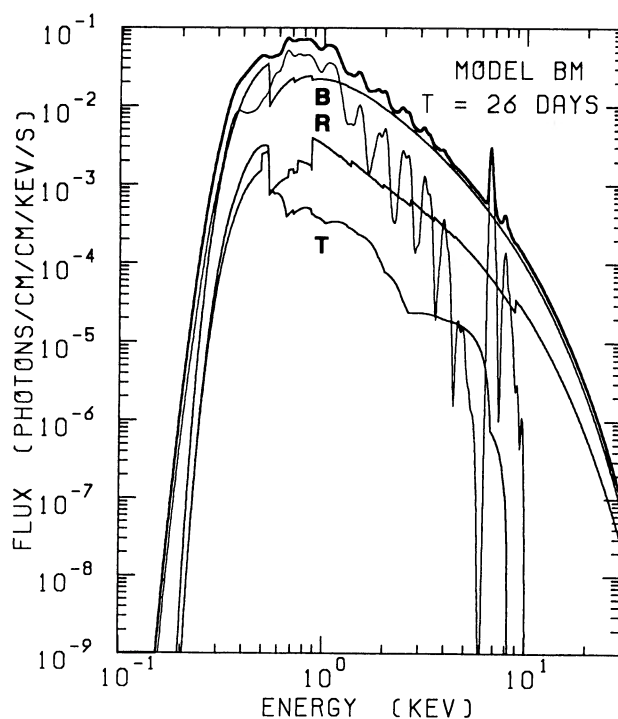


FIG. 7b

FIG. 7.—Same as Fig. 2b, but at  $t = 26$  days in (a) model B and (b) model Bm

dicts copious X-ray emission during the secondary light maximum; such an emission provides an observational test for the model.

If Gratton's model is correct, it is very likely that the material at a distance of 250 AU is ejecta of the previous outburst(s), since this type of secondary brightening was observed at both outbursts. The material is probably formed by a slow stellar wind having an expansion velocity of  $\sim 20 \text{ km s}^{-1}$  (e.g., Kato and Hachisu 1988), which is obtained by taking account of the interval between the two outbursts. Therefore, if the copious X-ray emission is confirmed, then it may pose a clue to the outburst mechanism of recurrent novae.

In the 1985 outburst of RS Ophiuchi discussed above, X-ray observations were performed on six occasions, ending 250 days after the optical light maximum (Mason *et al.* 1987). These observations showed no evidence for secondary brightening. The soft X-ray flux measured on the final occasion lies above the extrapolation of the earlier measurements. This might be due to the collision of the blast shock with a relatively dense ambient medium. However, there was no accompanying enhancement of the radio emission around that time (see Hjellming *et al.* 1986), as would be expected if the nonthermal radio emission is due to the particle acceleration near the blast-shock front. Alternatively, the soft X-rays observed on the final occasion may have originated primarily on the surface of the erupted white dwarf which had a temperature of  $3.5 \times 10^5 \text{ K}$  (Mason *et al.* 1987). If this is the case, there remains a possibility that RS Ophiuchi will flare up in the near future. We note in passing that if the shell is dusty the flaring may also occur at infrared wavelengths owing to the collisional heating of the dust grains by the shocked gas, as has been predicted for the remnant of SN 1987A (Itoh 1988).

In the 1989 outburst of V745 Scorpii, spectroscopic observations indicated the presence of tenuous material near the nova (Duerbeck and Schwarz 1989). This material might be a wind from the companion star or slow ejecta from the previous outburst(s). In any case, however, positive detection of the expected X-ray emission is hindered by the presence of a bright X-ray source in the vicinity of the nova (Makino 1989).

The X-ray and radio flares, and possibly the infrared flare also, may be observed first in T Pyxidis. This system underwent recorded outbursts in 1890, 1902, 1920, 1944, and 1966. It is very likely that the next outburst will occur soon. Further, a slowly expanding shell has been detected around that stellar system (see Shara *et al.* 1989 and references therein). The next outburst of this nova will provide an opportunity for coordinated observations at various wavelengths to test our predictions.

Future investigations of the dynamical evolution and non-equilibrium X-ray emission of a recurrent-nova remnant should take account of the asphericity of the remnant. An  $H\alpha + [N \text{ II}]$  photograph of T Coronae Borealis has shown that the nebular remnant consists mainly of two condensations on either side of the stellar system (Williams 1977). Similarly, the Very Long Baseline Interferometry observations of RS Ophiuchi during the 1985 outburst have shown two extensions on either side of the central bright feature (Hjellming *et al.* 1986; Porcas, Davis, and Graham 1987; Taylor *et al.* 1989). Further, the Balmer-line profiles of U Scorpii and V394 Coronae Austrinae during the 1987 outbursts indicate deficiencies of the ejecta moving in the plane of the sky (Sekiguchi *et al.* 1988, 1989). The expansion of the ejecta may be significantly impeded in that plane by the accretion disk around the erupted star (Sekiguchi *et al.* 1988), as has been proposed for

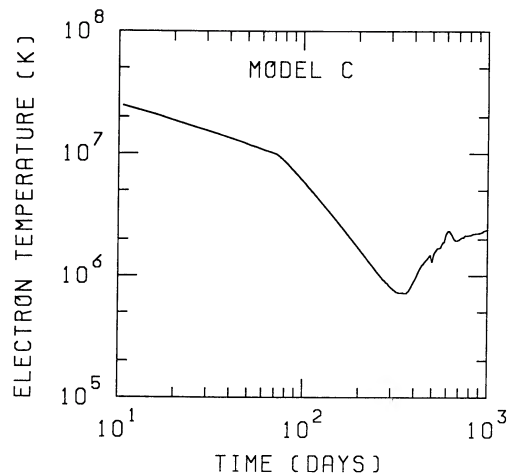


FIG. 8a

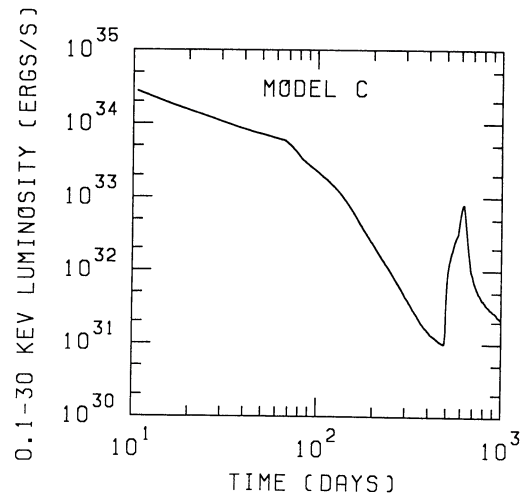


FIG. 8b

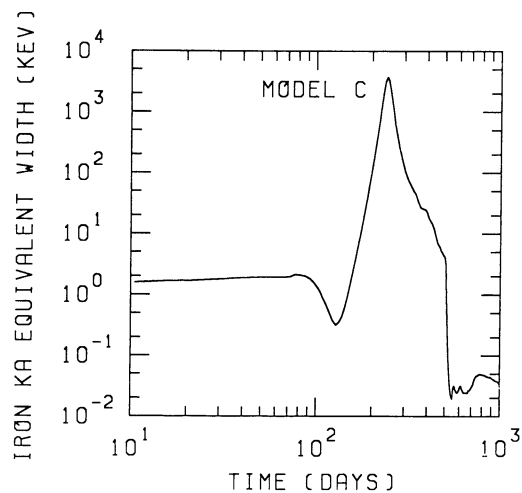


FIG. 8c

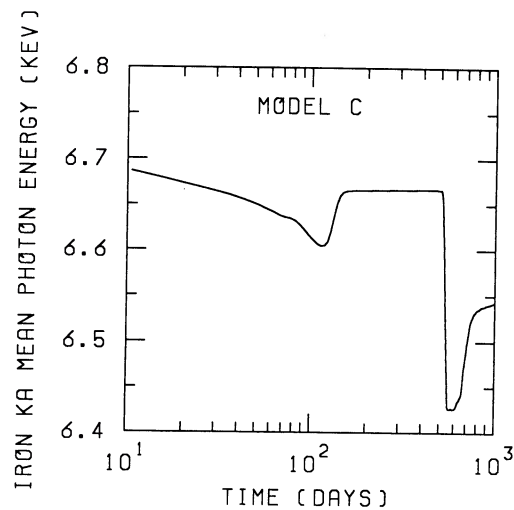


FIG. 8d

FIG. 8.—Same as Figs 3a, 3b, 3c, and 3d, but in model C

classical novae (Sparks and Starrfield 1973). Alternatively, the mass ejection itself may be bipolar. The CBM in these systems may also be aspherical owing to the orbital motion of the red-giant companion, as mentioned in § II. Thus aspherical expansions occur in almost all observed recurrent novae, although the degree of asphericity varies markedly among them.

#### V. CONCLUSIONS

When the ejecta of a recurrent nova collide with the dense CBM which has been formed by a wind from the red-giant companion, the blast-shocked CBM emits copious thermal X-rays. After the blast shock breaks out of the CBM, the CBM cools substantially by adiabatic expansion. As a result, the X-ray emission declines steeply, the shape of the X-ray spectrum softens, and the recombination lines and continua become prominent in the X-ray spectrum. The recurrent-nova remnant may be rejuvenated when it collides with the dense

shell which has been ejected slowly during the previous outburst(s). The collision is accompanied by X-ray and radio flares, and possibly by an infrared flare also. These signatures may be detected in the next outburst of T Pyxidis, which is very likely to occur in a few years. They may also be detected shortly in RS Ophiuchi and U Scorpii, which underwent their latest outbursts in 1985 and 1987, respectively.

The authors are grateful to K. Masai for providing his X-ray spectral code, to M. Arnaud for correspondence on the ionization and recombination coefficients, and to A. C. Sterling for a critical reading of the typescript and for comments. Numerical calculations were carried out at the Data Processing Center of Kyoto University, at the Space Data Analysis Center of the Institute of Space and Astronautical Science, and at the Astronomy Data Analysis Center of the National Astronomical Observatory (Japan). This work has been supported in part by the Japanese Ministry of Education, Science, and Culture (63540196).

## REFERENCES

- Allen, C. W. 1973, *Astrophysical Quantities* (3d ed.; London: Athlone), p. 31.
- Arnaud, M., and Rothenflug, R. 1985, *Astr. Ap. Suppl.*, **60**, 425.
- Bame, S. J., Asbridge, J. R., Gosling, J. T., Halbig, M., Paschmann, G., Skopke, N., and Rosenbauer, H. 1979, *Space Sci. Rev.*, **23**, 75.
- Band, D. L., and Liang, E. P. 1988, *Ap. J.*, **334**, 266.
- Bode, M. F. 1987, in *RS Ophiuchi (1985) and the Recurrent Nova Phenomenon*, ed. M. F. Bode (Utrecht: VNU Science Press), p. 241.
- Bode, M. F., and Kahn, F. D. 1985, *M.N.R.A.S.*, **217**, 205.
- Brecher, K., Ingham, W. H., and Morrison, P. 1977, *Ap. J.*, **213**, 492.
- Callus, C. M., Evans, A., and Albinson, J. S. 1986, *Irish Astr. J.*, **17**, 330.
- Chevalier, R. A., and Liang, E. P. 1989, *Ap. J.*, **344**, 332.
- Dickel, J. R., and Jones, E. M. 1985, *Ap. J.*, **288**, 707.
- Duerbeck, H. W., and Schwarz, H. E. 1989, *IAU Circ.*, No. 4825.
- Evans, A. 1987, in *RS Ophiuchi (1985) and the Recurrent Nova Phenomenon*, ed. M. F. Bode (Utrecht: VNU Science Press), p. 117.
- Friedjung, M. 1987, in *RS Ophiuchi (1985) and the Recurrent Nova Phenomenon*, ed. M. F. Bode (Utrecht: VNU Science Press), p. 77.
- Gratton, L. 1952, *Transactions IAU*, **VIII**, 849.
- Hjellming, R. M., van Gorkom, J. H., Taylor, A. R., Seaquist, E. R., Padin, S., Davis, R. J., and Bode, M. F. 1986, *Ap. J. (Letters)*, **305**, L71.
- Itoh, H. 1979, *Pub. Astr. Soc. Japan*, **31**, 541.
- . 1988, *Pub. Astr. Soc. Japan*, **40**, 263.
- . 1989, *Pub. Astr. Soc. Japan*, **41**, 853.
- Itoh, H., and Fabian, A. C. 1984, *M.N.R.A.S.*, **208**, 645.
- Itoh, H., Hayakawa, S., Masai, K., and Nomoto, K. 1987, *Pub. Astr. Soc. Japan*, **39**, 529.
- Itoh, H., and Masai, K. 1989, *M.N.R.A.S.*, **236**, 885.
- Itoh, H., Masai, K., and Nomoto, K. 1988, *Ap. J.*, **334**, 279.
- Kato, M., and Hachisu, I. 1988, *Ap. J.*, **329**, 808.
- Kenyon, S. J. 1986, *The Symbiotic Stars* (Cambridge: Cambridge University Press), pp. 91–97 and 181–186.
- Livio, M., Truran, J. W., and Webbink, R. F. 1986, *Ap. J.*, **308**, 736.
- Makino, F. 1989, *IAU Circ.*, No. 4825.
- Masai, K., Hayakawa, S., Inoue, H., Itoh, H., and Nomoto, K. 1988, *Nature*, **335**, 804.
- Masai, K., Hayakawa, S., Itoh, H., and Nomoto, K. 1987, *Nature*, **330**, 235.
- Mason, K. O., Córdoba, F. A., Bode, M. F., and Barr, P. 1987, in *RS Ophiuchi (1985) and the Recurrent Nova Phenomenon*, ed. M. F. Bode (Utrecht: VNU Science Press), p. 167.
- McKee, C. F. 1974, *Ap. J.*, **188**, 335.
- Mewe, R., Gronenschild, E. H. B. M., and van den Oord, G. H. J. 1985, *Astr. Ap. Suppl.*, **62**, 197.
- O'Brien, T. J., and Kahn, F. D. 1987, *M.N.R.A.S.*, **228**, 277.
- O'Brien, T., Kahn, F. D., and Bode, M. F. 1987, in *RS Ophiuchi (1985) and the Recurrent Nova Phenomenon*, ed. M. F. Bode (Utrecht: VNU Science Press), p. 177.
- Ögelman, H., Krautter, J., and Beuermann, K. 1987, *Astr. Ap.*, **177**, 110.
- Porcas, R. W., Davis, R. J., and Graham, D. A. 1987, in *RS Ophiuchi (1985) and the Recurrent Nova Phenomenon*, ed. M. F. Bode (Utrecht: VNU Science Press), p. 203.
- Pottasch, S. R. 1967, *Bull. Astr. Inst. Netherlands*, **19**, 227.
- Richtmyer, R. D., and Morton, K. W. 1967, *Difference Methods for Initial-Value Problems* (2d ed.; New York: Interscience), p. 317.
- Rosino, L. 1987, in *RS Ophiuchi (1985) and the Recurrent Nova Phenomenon*, ed. M. F. Bode (Utrecht: VNU Science Press), p. 1.
- Sekiguchi, K., Catchpole, R. M., Fairall, A. P., Feast, M. W., Kilkenny, D., Laney, C. D., Evans, T. L., Marang, F., and Parker, Q. A. 1989, *M.N.R.A.S.*, **236**, 611.
- Sekiguchi, K., Feast, M. W., Whitelock, P. A., Overbeek, M. D., Wargau, W., and Jones, J. S. 1988, *M.N.R.A.S.*, **234**, 281.
- Shara, M. M. 1989, *Pub. Astr. Soc. Pacific*, **101**, 5.
- Shara, M. M., Moffat, A. F. J., Williams, R. E., and Cohen, J. G. 1989, *Ap. J.*, **337**, 720.
- Snijders, M. A. J. 1987, in *RS Ophiuchi (1985) and the Recurrent Nova Phenomenon*, ed. M. F. Bode (Utrecht: VNU Science Press), p. 51.
- Sparks, W. M., and Starrfield, S. 1973, *M.N.R.A.S.*, **164**, 1P.
- Sparks, W. M., Starrfield, S., and Truran, J. W. 1978, *Ap. J.*, **220**, 1063.
- Spitzer, L., Jr. 1962, *Physics of Fully Ionized Gases* (2d ed.; New York: Interscience), p. 131.
- Starrfield, S. 1988, in *Multiwavelength Astrophysics*, ed. F. A. Córdoba (Cambridge: Cambridge University Press), p. 159.
- Taylor, A. R., Davis, R. J., Porcas, R. W., and Bode, M. F. 1989, *M.N.R.A.S.*, **237**, 81.
- Webbink, R. F. 1976, *Nature*, **262**, 271.
- Webbink, R. F., Livio, M., Truran, J. W., and Orio, M. 1987, *Ap. J.*, **314**, 653.
- Williams, R. E. 1977, in *IAU Colloquium 42, The Interaction of Variable Stars with Their Environment*, ed. R. Kippenhahn, J. Rahe, and W. Strohmeier (Bamberg: Reims Sternwarte), p. 242.

IZUMI HACHISU: Department of Aeronautical Engineering, Kyoto University, Kyoto 606, Japan

HIROSHI ITOH: Department of Astronomy, Faculty of Science, Kyoto University, Kyoto 606, Japan